Effect of Channel Noise on Fractionally Spaced CMA and MMA

Jenq-Tay Yuan[1], *Senior Member*, *IEEE*, Jen-Hung Chao[2], and Tzu-Chao Lin[3]
[1,3]Graduate Institute of Applied Science and Engineering, [2]Department of Electrical Engineering,
Fu Jen Catholic University, Taipei 24205, Taiwan, R.O.C.
E-mail: [1]yuan@ee.fju.edu.tw, [2]allen_hua10@hotmail.com,[3]tclin@ee.fju.edu.tw

***Abstract*—This paper analyzes and compares the robustness of the constant modulus algorithm (CMA) and multimodulus algorithm (MMA) in the presence of additive channel noise when the channel satisfies the zero-forcing conditions. A generalized formulation of the relocation of stationary points toward the origin in terms of signal-to-noise ratio (SNR) was developed for both the CMA and the MMA to facilitate the comparison of the sensitivity to channel noise of CMA with that of MMA for various source constellations. Relationships between the relocation of the stationary points for the MMA and CMA were derived. Simulation results appear to confirm the main results of this work, regarding the sensitivity to channel noise when the fractionally spaced CMA (FS-CMA) and fractionally spaced MMA (FS-MMA) criteria were applied with various sources.**

***Index Terms*—Additive channel noise, blind equalization, constant modulus algorithm (CMA), fractionally spaced equalizers (FSE), multimodulus algorithm (MMA).**

I. INTRODUCTION

The constant modulus algorithm (CMA) is an extensively adopted blind equalization algorithm [1]–[3]. Although the fact that the CMA is carrier phase independent has been widely regarded as one key benefit of the CMA when it is practically implemented in blind adaptive receivers [4], a phase rotator that can rotate the constellation back into the right position is needed in steady-state operation, increasing the complexity of the implementation of the receiver. Recently, the multimodulus algorithm (MMA) [5]–[8] has attracted interest from researchers in the field of blind equalization since it allows simultaneous joint blind equalization and carrier phase recovery, eliminating the need for an adaptive phase rotator to perform separate constellation phase recovery.

To demonstrate the robustness of the *fractionally spaced* (FS) CMA (FS-CMA) to additive channel noise, Fijalkow, Touzni, and Treichler [9] examined the effect of channel noise on the FS-CMA. They expressed the FS-CMA cost function in the presence of white additive channel noise and described the new cost-function minima in terms of signal-to-noise ratio (SNR) as a *perturbation* of the noise-free minima. Chung and LeBlanc [10] investigated the relocation of local minima of the FS-CMA cost function toward the origin owing to additive channel noise.

Previous analyses in [9] and [10] focus on the CMA and have mainly considered a one-dimensional real-valued phase-shift keying (BPSK) source. When the SNR approaches infinity, some two-dimensional source constellations are well known to become better suited to the CMA, whereas others may become better suited to the MMA [8]; both CMA and MMA require about the same computational cost. This work analytically investigates and compares the effects of additive channel noise on the FS-CMA and the FS-MMA, in terms of *relocation of stationary points* toward the origin when *various two-dimensional symmetric signal constellations* are used.

II. CHANNEL MODEL AND EQUALIZATION

A fractionally-spaced-equalizer (FSE) system is a single-input multiple-output (SIMO) discrete system model with a single complex input $s_n = s_R + js_I$ where s_R and s_I denote the real and imaginary parts of s_n, respectively. Consider an example of a *T/2*-spaced FSE used in [Fig. 5, 3], in which a complex-valued *T*-spaced symbol sequence $\{s_n\}$ is transmitted through a FS channel that divides these sequences into even and odd subchannels of length $2N_c$: c_i^{even} and c_i^{odd}, for $0 \le i \le N_c - 1$. The odd and even received signals that are corrupted by additive channel noise, w_n^{odd} and w_n^{even}, for $n = 0,1,2,\cdots$, are then filtered by the even and odd subequalizers of length $2N_f$, f_i^{even} and f_i^{odd}, for $0 \le i \le N_f - 1$, respectively. The equalizer output y_n that is used to estimate s_n can be obtained by

$$y_n = \mathbf{f}^T\mathbf{C}^T\mathbf{s}(n) + \mathbf{f}^T\mathbf{w}(n) = \mathbf{h}^T\mathbf{s}(n) + \mathbf{f}^T\mathbf{w}(n) \quad (1)$$

where $\mathbf{s}(n) = [s_n, s_{n-1}, \cdots, s_{n-N+1}]^T$, $\mathbf{C}$ is a $N \times (2N_f)$ complex FS convolution matrix in which $N = N_c + N_f - 1$ [3]; $\mathbf{w}(n) = [w_n^{even}, w_n^{odd}, w_{n-1}^{even}, w_{n-1}^{odd}, \cdots, w_{n-N_f+1}^{even}, w_{n-N_f+1}^{odd}]^T$ and $\mathbf{f}^T = [f_0^{odd}, f_0^{even}, \cdots, f_{N_f-1}^{odd}, f_{N_f-1}^{even}]$. Notably, vector $\mathbf{h}$ in (1) can be expressed as $\mathbf{h} = [h_0, h_1, \cdots, h_{N-1}]^T \triangleq [h_0(n), h_1(n), \cdots, h_{N-1}(n)]^T = \mathbf{Cf}$, which is the *N*-length complex *combined channel-equalizer* impulse response (IR) vector with M arbitrarily located non-zero components at time, *n*, during the blind equalization process and $M \le N$, where $M = 1,2,3,\cdots$. When channel noise is not present, perfect equalization may be achievable under the following two well-known conditions, known as the zero-forcing (ZF) conditions [3], [9]: (i) $2N_f \ge N_c + N_f - 1$; (ii) the two subchannels have no common roots. Hereafter, both (i) and (ii) are assumed to be satisfied.

When there is no possibility of confusion, the notation is simplified by suppressing the time index, *n*, e.g., $s_n \triangleq s$ and $y_n \triangleq y$. In order to ease the analysis, the following assumptions are made: (**A1**) s is a complex symmetric identically independent distributed (i.i.d.) source, zero-mean with second central moment $m_2 = E[|s|^2] = 1$ and fourth central moment $m_4 = E[|s|^4]$, where $E[.]$ denotes the statistical expectation. (**A2**) The *kurtosis deviation* of s is defined as $\eta_s = 2m_2^2 - m_4 = m_2^2(2 - k_s)$, where $k_s = m_4 / m_2^2 = m_4$ is the kurtosis of s. All of the complex sources that are considered in this work are sub-Gaussian such that $k_s < 2$ (or $\eta_s > 0$). (**A3**) w_n^{even} and w_n^{odd} are assumed to be a Gaussian white, zero-mean, complex-valued rotationally invariant noise with power $E[|w_n^{even}|^2] = E[|w_n^{odd}|^2] = \sigma_w^2$ such that $E[(w_n^{even})^i] = E[(w_n^{odd})^i] = 0$, $i = 1,2,3,\cdots$ [3, pp. 1945], and they are assumed to be uncorrelated with the source.

Since quadrature amplitude modulation (QAM) cross constellations (such as Cross 128-QAM [6]) and modified QAM constellations (such as 16-point V.29 [11], and 96-point V.34 modem [12]) are also of interest, s_R and s_I cannot be assumed to be mutually independent. Accordingly, the second cross-moment may be expressed as $E[s_R^2 s_I^2] = \gamma E[s_R^2]E[s_I^2]$, in which $\gamma = 1$ for square QAM, and $0 < \gamma < 1$ for most other constellations. Notably, the fourth-order statistic, $E[s^4]$, which is absent in the CMA cost function but plays a crucial role in the MMA, can be expressed as $E[s^4] = m_4 - 8E[s_R^2 s_I^2] = m_4 - 2\gamma$. This study investigates the effect of channel noise on both the CMA and the MMA in the combined channel-equalizer (**h**) space rather than the equalizer (**f**) space, because studying their cost functions as a function of **h** is more convenient than studying them as a function of **f**.

978-1-4673-1881-5/12/$31.00 ©2012 IEEE

III. Relocation of Stationary Points of Noisy CMA

This section investigates the relocation of stationary points of the CMA toward the origin when channel noise is present. First, the CMA cost function with a complex source is

$$J_{CMA} = E[(|y|^2 - R_2)^2] = E[|y|^4] - 2R_2 E[|y|^2] + R_2^2 \qquad (2)$$

where $R_2 = m_4 / m_2 = m_4$. Substituting (1) into (2) and using assumptions (A1)–(A3) yield

$$\begin{aligned} J_{CMA} = & \underbrace{m_4(\|\mathbf{h}\|^2 - 1)^2 + R_2^2 - m_4 + \eta_s I_h}_{J_0(\mathbf{h})} \\ & + \underbrace{2\sigma_w^2 \|\mathbf{C}^{-1}\mathbf{h}\|^2 (2\|\mathbf{h}\|^2 - R_2 + \sigma_w^2 \|\mathbf{C}^{-1}\mathbf{h}\|^2)}_{J_w(\mathbf{h})} \end{aligned} \qquad (3)$$

where $J_0(\mathbf{h})$ is the *noise-free* cost function and $J_w(\mathbf{h})$ is the *noise-related* cost function. The inter-symbol interference (ISI) of the combined channel equalizer is defined as

$$I_h \triangleq \sum_{i \neq j}^{N-1} |h_i|^2 |h_j|^2 = \|\mathbf{h}\|^4 - \sum_{i=0}^{N-1} |h_i|^4 \qquad (4)$$

in which $h_i = r(i)e^{j\theta(i)} = r(i)\cos\theta(i) + jr(i)\sin\theta(i)$, $0 \le i \le N-1$, where $\theta(i)$, $0 \le i \le N-1$, are the phases of the combined channel-equalizer impulse responses, h_i , and they are related to the phase offset introduced by a channel owing to $\mathbf{h} = [h_0, h_1, \cdots, h_{N-1}]^T = \mathbf{Cf}$. $\|\mathbf{f}\|^2 = \|\mathbf{C}^{-1}\mathbf{h}\|^2 = \mathbf{h}^H \mathbf{C}^{-H}\mathbf{C}^{-1}\mathbf{h}$ in (3) can be computed as

$$\begin{aligned} \|\mathbf{C}^{-1}\mathbf{h}\|^2 = & \underbrace{\sum_{i=0}^{N-1} \rho_{i,i} r^2(i)}_{D} \\ & + \underbrace{\sum_{i=1}^{N-1} \sum_{j=0}^{i-1} 2\rho_{i,j} r(i) r(j) \cos[\theta(i) - \theta(j) - \phi_{i,j}]}_{\Gamma} \triangleq D + \Gamma \end{aligned} \qquad (5)$$

in which $\rho_{i,j}$ (magnitude) and $\phi_{i,j}$ (phase rotation) are defined in terms of $d_{i,j} = \rho_{i,j} e^{j\phi_{i,j}}$, $i, j = 0, 1, ..., N-1$, where $d_{i,j}$ are elements of the $N \times N$ matrix $\mathbf{C}^{-H}\mathbf{C}^{-1}$. Γ in (5) represents the combined effect of both the ISI and the phase distortion introduced by channel.

In order to make the analysis tractable, the following assumption (A4) and approximation (A5) are made. (**A4**) Large or moderate SNR (not-too-great σ_w^2) is assumed. This assumption has also been made in [9], because if SNR is low, then J_{CMA} in (3) will be dominated by the noise-related part, $J_w(\mathbf{h})$. As a result, the analytical solution would not be a meaningful expression for the minima. Hence, we focus on the case when SNR is large or moderate. (**A5**) Γ decreases rapidly and may become very small in (5) once blind equalization starts (i.e., $\|\mathbf{C}^{-1}\mathbf{h}\|^2 \cong D$). To justify the validity of this approximation, simulation results in Fig. 1 demonstrate how each non-zero component (in terms of $r(l) \triangleq |h_l|, 0 \le l \le N-1$) of the combined channel-equalizer vector $\mathbf{h} = [h_0, h_1, \cdots, h_{N-1}]^T$ dynamically evolves during the blind equalization process at various iterations. During the simulations, CMA was used and a sequence of 16-QAM symbols was transmitted through a three-ray multipath channel proposed in [15]; white Gaussian noise was also added so that the final SNR was 30dB. At the beginning of the equalization process (e.g., at the 20-th iteration), a non-zero component of **h** with maximum magnitude increased rapidly while the remaining nonzero components with small magnitude decreased. The non-zero component of **h** with maximum magnitude continued to dominate at the 50-th, 100-th, and 200-th iteration while the remaining nonzero components continued to decrease. After the 200-th iteration, the blind equalization process was approaching steady state ($M \to 1$), and the non-zero component of **h** with maximum magnitude was approaching 1 while the remaining nonzero components of **h** were approaching zero. Figure 1, a typical simulation result using the CMA (or the MMA), demonstrates that once blind equalization starts with a good gradient-descent initialization and appropriate step-sizes, a non-zero component of **h** with maximum magnitude, $r(k)$, stands out, and the remaining $M-1$ nonzero components, $r(l), l \neq k$, fall rapidly, eventually diminishing to zero. Therefore, Γ may decrease rapidly once blind equalization starts. Under (A4) and (A5), terms such as $\sigma_w^2\Gamma$, $\sigma_w^4\Gamma$ and $\sigma_w^4\Gamma^2$, in (3), may be ignored. The CMA cost function in (3) reduces to

$$J_{CMA} = m_4\left(\|\mathbf{h}\|^2 - 1\right)^2 + R_2^2 - m_4 + \eta_s I_h + 2\sigma_w^2 D\left(2\|\mathbf{h}\|^2 - R_2 + \sigma_w^2 D\right)$$

Stationary points of the noisy CMA may thus be located using $\partial J_{CMA} / \partial r(k) = 0$, $0 \le k \le M-1$, for each non-zero component of **h**, to solve *M* simultaneous equations. It is well known that all of the CMA stationary points (except the one at the origin) in the *noise-free* case are located on a *single connected circle* with a common radius *r* for each element of **h** when complex source constellations are used [8], [13]. To obtain mathematically tractable results in the presence of additive channel noise, an idea first introduced by Chung and LeBlanc [10] is adopted by making the following assumption. (**A6**) $\mathbf{h} = r\mathbf{h}'$ such that $\|\mathbf{h}\|^2 = r^2\|\mathbf{h}'\|^2$, where $\mathbf{h}' = [h'_0, h'_1, \cdots, h'_{N-1}]^T = [r'(0)e^{j\theta(0)}, r'(1)e^{j\theta(1)}, \cdots, r'(N-1)e^{j\theta(N-1)}]^T$ and $0 < r \le 1$ represents a *common shrinking in the distances* between the stationary points of each component of **h** and the origin, owing to the effect of *channel noise* and *ISI*. As a result of (A6), $\|\mathbf{h}'\|^2 = 1$ when $M \ge 1$ (during both the transient stage and the steady-state). This is because the effect of both channel noise and ISI has been taken into account by *r*. As a result of (A6), the *M* simultaneous equations $\partial J_{CMA} / \partial r(k) = 0$, for $0 \le k \le M-1$, which can be solved for the location of the CMA stationary points for *each non-zero component* of **h**, can thus be reduced to a single equation in the noisy case, which is solved by setting $\partial J_{CMA} / \partial r = 0$, regardless of the value of *M* . The CMA cost function may thus be expressed as

$$\begin{aligned} J_{CMA}(r\mathbf{h}') = & (2\sigma_w^4 D'^2 + 4\sigma_w^2 \|\mathbf{h}'\|^2 D' + R_2 \|\mathbf{h}'\|^4 \\ & + \eta_s I_{h'}) r^4 - 2R_2(\|\mathbf{h}'\|^2 + \sigma_w^2 D') r^2 + R_2^2 \end{aligned} \qquad (6)$$

which is a quadratic function of r^2 , where $I_{h'} = (1/r^4) I_h$,

$$D' \triangleq (1/r^2) \cdot D \cong \|\mathbf{C}^{-1}\mathbf{h}'\|^2 \qquad (7)$$

The set of CMA stationary points for $M \ge 1$ can thus be obtained by first setting

$$\begin{aligned} \partial J_{CMA}(r\mathbf{h}')/\partial r = 4r\{ & (m_4 + 4\sigma_w^2 D' + 2\sigma_w^4 D'^2 + \eta_s I_{h'}) r^2 \\ & - R_2(1 + \sigma_w^2 D')\} = 0 \end{aligned} \qquad (8)$$

applying (6) in the presence of additive channel noise as well as ISI to compute their common shrinking, *r*. When $r \neq 0$, using $\eta_s = 2 - m_4$ and $R_2 = m_4$ yields

$$r = \sqrt{R_2(1 + \sigma_w^2 D') / \left(2(1 + \sigma_w^2 D')^2 - \eta_s(1 - I_{h'})\right)} \qquad (9)$$

In the presence of noise and ISI ($M \ge 2$), by using $I_{h'} = \sum_{i \neq j} |h'_i|^2 |h'_j|^2 = \|\mathbf{h}'\|^4 - \sum_i |h'_i|^4 = 1 - \sum_i r'(i)^4 = 1 - (1/M)$, *r* in (10) can also be expressed as

$$r = \sqrt{(2 - \eta_s)(1 + \sigma_w^2 D') / \left(2(1 + \sigma_w^2 D')^2 - \eta_s / M\right)} < 1 \qquad (10)$$

In deriving (10), $r'(0) = r'(1) = \cdots = r'(M-1) = \sqrt{1/M}$ is set to satisfy $\|\mathbf{h}'\|^2 = 1$ and to ensure that all of the stationary points are located on *one single connected circle* for $M \ge 1$.

IV. Relocation of Stationary Points of Noisy MMA

The MMA cost function with complex source is expressed as [5]–[8]

$$\begin{aligned} J_{MMA} = & E[(y_R^2 - R_{2,R})^2] + E[(y_I^2 - R_{2,I})^2] \\ = & E[y_R^4] + E[y_I^4] - 2R_{2,R}(E[y_R^2] + E[y_I^2]) + 2R_{2,R}^2 \end{aligned} \qquad (11)$$

where $R_{2,R} = E[s_R^4] / E[s_R^2] = R_{2,I}$ for symmetric constellations. Substituting (1) into (11) and using (A1)–(A3) yield

$$J_{MMA}=\underbrace{\tfrac{1}{4}\{E[s^4]\cdot\sum|h_i|^4\cos 4\theta(i)\}+\tfrac{3}{4}\{m_4\|\mathbf{h}\|^4+\eta_s I_h\}-2R_{2,R}\|\mathbf{h}\|^2+2R_{2,R}^2}_{J_0(\mathbf{h})}+\underbrace{2\sigma_w^2\|\mathbf{C}^{-1}\mathbf{h}\|^2\left(\tfrac{3}{2}\|\mathbf{h}\|^2-R_{2,R}+\tfrac{3}{4}\sigma_w^2\|\mathbf{C}^{-1}\mathbf{h}\|^2\right)}_{J_w(\mathbf{h})} \quad (12)$$

where $\theta(i)$, $0\le i\le N-1$, are the phases of $h_i=r(i)e^{j\theta(i)}$, $0\le i\le N-1$, defined in $\mathbf{h}=[h_0,h_1,\cdots,h_{N-1}]^T=\mathbf{Cf}$, and $J_0(\mathbf{h})$ is the *noise-free* cost function and $J_w(\mathbf{h})$ is the *noise-related* cost function. $E[s^4]\cdot\sum_i|h_i|^4\cos 4\theta(i)$ in (12), related to the *fourth-order statistic*, $E[s^4]$, contains the phase information of the blind equalizer output and is absent from the CMA cost function given by (3). It reveals the major difference between the CMA and the MMA.

A. Relocation of stationary points of MMA in angular direction

When additive channel noise is present, the stationary points of the noisy MMA in the combined channel-equalizer (**h**) space can be found by setting the gradient of J_{MMA} in (12) to zero, such that $\nabla J_{MMA}=\mathbf{r}\,\partial J_{MMA}/\partial r(k)+(\boldsymbol{\theta}/r(k))\cdot\partial J_{MMA}/\partial\theta(k)=0$. First, consider the location of the stationary points along $\theta(k)$ (angular direction) by setting $\partial J_{MMA}/\partial\theta(k)=0$, $0\le k\le N-1$, yielding $\partial[J_0(\mathbf{h})+J_w(\mathbf{h})]/\partial\theta(k)=0$, $0\le k\le N-1$. To simplify the computation, $J_0(\mathbf{h})$ and $J_w(\mathbf{h})$ are considered separately, i.e., $\partial J_0(\mathbf{h})/\partial\theta(k)=0$ and $\partial J_w(\mathbf{h})/\partial\theta(k)=0$.

(i). The *noise-free* case:

As has been derived in [7], $\partial J_0(\mathbf{h})/\partial\theta(k)=0$, giving $E[s^4]\{-r^4(k)[\sin 4\theta(k)]\}=0$, yields $\theta(k)\in\{0,\pi/4,\pi/2,3\pi/4,\pi,5\pi/4,3\pi/2,7\pi/4\}$, for $0\le k\le N-1$ (since $E[s^4]\ne 0$) when $r(k)\ne 0$, which explicitly specifies the location of the stationary points of the *noise-free MMA* in the $\theta(k)$ direction.

(ii). The *noise-related* case:

The effect of noise on $\theta(k)$ is then considered by setting $\partial J_w(\mathbf{h})/\partial\theta(k)=0$. By using both (A4) and (A5), the noise-related cost function $J_w(\mathbf{h})$ in (12) reduces to

$$J_w(\mathbf{h})=2\sigma_w^2 D(\tfrac{3}{2}\|\mathbf{h}\|^2-R_{2,R})+\tfrac{3}{2}\sigma_w^4 D^2$$

which turns out to be independent of $\theta(k)$, $0\le k\le N-1$. Accordingly, the stationary points of the MMA do not relocate in the *angular direction* by channel noise.

B. Relocation of stationary points of MMA in radial direction

The radial components, $r(k)$, of the stationary points of the noisy MMA are now determined. As in the derivation of the noisy CMA case, the following two approximations are made. In the first approximation, **h** may be expressed as $\mathbf{h}=r_+\mathbf{h}'$ when $\theta(k)\in\{0,\pi/2,\pi,3\pi/2\}$ such that $\cos 4\theta(k)=1$ in (12). Consequently, the effect of channel noise and ISI may be taken into account by r_+ in $\mathbf{h}=r_+\mathbf{h}'$ with $\|\mathbf{h}'\|^2=1$. Equation (12) may thus be expressed as

$$J_{MMA}(r_+\mathbf{h}')=\left\{\tfrac{1}{4}E[s^4]\cdot(\|\mathbf{h}'\|^4-I_{h'})+\tfrac{3}{4}\left(m_4\|\mathbf{h}'\|^4+2\sigma_w^4D'^2+4\sigma_w^2\|\mathbf{h}'\|^2D'+\eta_s I_{h'}\right)\right\}r_+^4-2R_{2,R}(\|\mathbf{h}'\|^2+\sigma_w^2D')r_+^2+2R_{2,R}^2$$

where $I_h=r_+^4 I_{h'}$; D' is defined in (7). To locate the stationary points of the noisy MMA along $\theta(k)\in\{0,\pi/2,\pi,3\pi/2\}$, $\partial J_{MMA}(r_+\mathbf{h}')/\partial r_+=0$ is set, yielding (similar to the derivation of (9))

$$r_+=\sqrt{2R_{2,R}(1+\sigma_w^2D')\big/\left[3(1+\sigma_w^2D')^2+(2m_4-\gamma-3)\cdot(1-I_{h'})\right]} \quad (13)$$

In the second approximation, **h** may be expressed as $\mathbf{h}=r_-\mathbf{h}'$ when $\theta(k)\in\{\pi/4,3\pi/4,5\pi/4,7\pi/4\}$ such that $\cos 4\theta(k)=-1$ in (12). The location of the stationary points of the noisy MMA along $\theta(k)\in\{\pi/4,3\pi/4,5\pi/4,7\pi/4\}$ can be computed to be

$$r_-=\sqrt{2R_{2,R}(1+\sigma_w^2D')\big/\left[3(1+\sigma_w^2D')^2+(m_4+\gamma-3)\cdot(1-I_{h'})\right]} \quad (14)$$

It is worth noting that $r_-\ne r_+$ even in the noise-free case [8].

Unlike the CMA, which is independent of $E[s^4]$, both r_+ and r_- in the MMA are affected by whether it uses sources with $E[s^4]>0$ (such as V.29 and 4-phase-shift keying (4-PSK)) or $E[s^4]<0$ (such as square 256-QAM and cross 128-QAM). When $\sigma_w^2=0$ and $I_{h'}=0$ (ISI-free and $M=1$), $r_+=\sqrt{2R_{2,R}/(3+2m_4-\gamma-3)}=1$, and $r_-=\sqrt{2R_{2,R}/(3+m_4+\gamma-3)}=\sqrt{[(m_4+\gamma)+m_4-2\gamma]/(m_4+\gamma)}$, where $R_{2,R}=m_4-\gamma/2$. In this noise-free and ISI-free scenario with source $E[s^4]=m_4-2\gamma>0$, $r_->r_+=1$ and, therefore, r_- must be normalized by applying $G\triangleq\sqrt{(2m_4-\gamma)/(m_4+\gamma)}$ such that $r_-/G=1$, to produce the output signal constellation of the MMA without amplification, because r_- and r_+ correspond to the locations of the *global minima* and saddle points, respectively. However, in the noise-free and ISI-free case with source $E[s^4]=m_4-2\gamma<0$, the above normalization becomes unnecessary because $r_-<r_+=1$, where r_+ and r_- correspond to the locations of the *global minima* and saddle points, respectively.

In the presence of additive channel noise and ISI, $|h'_0|=|h'_1|=\cdots=|h'_{M-1}|=\sqrt{1/M}$, $M\ge 1$, to satisfy $\|\mathbf{h}'\|^2=1$, and, therefore, $I_{h'}=1-(1/M)$, which can be substituted into (13) and (14), respectively, to yield

$$r_+=\sqrt{2R_{2,R}(1+\sigma_w^2D')\big/\left[3(1+\sigma_w^2D')^2+(2m_4-\gamma-3)\cdot(1-I_{h'})\right]} \quad (15)$$

and

$$r_-=\sqrt{2R_{2,R}(1+\sigma_w^2D')\big/\left[3(1+\sigma_w^2D')^2+(m_4+\gamma-3)\cdot(1-I_{h'})\right]} \quad (16)$$

C. Sensitivity to channel noise

To facilitate the comparison of sensitivity to additive channel noise when using both CMA and MMA with various source constellations, we formulate both r_+ in (15) (for the MMA with sources such that $E[s^4]<0$) and r_-/G [using (16) and $G\triangleq\sqrt{(2m_4-\gamma)/(m_4+\gamma)}$] (for the MMA with sources such that $E[s^4]>0$) of the MMA, as well as r in (9) (by using $\eta_s=2-m_4$) of the CMA (for the CMA with all sources), all of which correspond to the *relocation* of potential local minima toward the origin owing to channel noise, can be expressed using the generalized formulation,

$$\sqrt{(1+\sigma_w^2D')\Big/\left(\tfrac{1}{M}+\tfrac{(1+\sigma_w^2D')^2-\frac{1}{M}}{Z}\right)}\triangleq R \quad (17)$$

for which Z may be set to be $Z\triangleq Z_{r_+}=(2m_4-\gamma)/3=\gamma+2E[s^4]/3$ (for MMA with sources such that $E[s^4]<0$), $Z\triangleq Z_{r_-}=(m_4+\gamma)/3=\gamma+E[s^4]/3$ (for MMA with sources such that $E[s^4]>0$), and $Z\triangleq Z_r=k_s/2=(E[s^4]/2)+\gamma$ (for CMA with all sources). In all the three cases, $Z>0$ can be straightforwardly verified; see also columns 5 and 6 of Table I. Clearly, for the same SNR, when both the CMA and the MMA use various constellations, a larger value of Z in (17) yields a smaller relocation owing to channel noise, and, consequently, a lower sensitivity of R in (17) to channel noise. This result follows from the fact that $(1+\sigma_w^2D')^2$ is the dominating term in (17), which determines the sensitivity to channel noise when both the CMA and the MMA are used. In summary, Z_r is related to Z_{r_-} and Z_{r_+} by

$$Z_r=Z_{r_v}+\left|E[s^4]\right|/6,\ \textit{where}\begin{cases}Z_{r_v}=Z_{r_-},\ \textit{for}\ E[s^4]>0\\ Z_{r_v}=Z_{r_+},\ \textit{for}\ E[s^4]<0\end{cases} \quad (18)$$

The following observations are obtained from (18).

Equation (18) indicates that the CMA is less sensitive to channel

noise than the MMA in terms of *equalization* for *all possible sources*, giving the CMA an advantage over the MMA when additive channel noise is present. More importantly, when the CMA is used as a standard to which the MMA with different sources can be compared, (18) reveals that when the MMA is used with a source with a smaller value of $|E[s^4]|$, its resistance to additive channel noise is closer to that of using the CMA, and, therefore, the MMA is less sensitive to channel noise. This result is in conflict with the existing result that a source with a larger value of $|E[s^4]|$ tends to be associated with more effective blind equalization and carrier phase recovery of the MMA *in the absence of channel noise* [8]. Consequently, $E[s^4]$, which is crucial in the built-in fourth-power phase estimator in the MMA, turns out to make the MMA more vulnerable to additive channel noise than the CMA. Since $E[s^4]=0$ when 8-PSK is used, (18) indicates that the MMA and the CMA are equally sensitive to additive channel noise when 8-PSK is used. Moreover, (17) along with $Z \triangleq Z_r = k_s/2$ reveals that when the CMA is used with various sources, a larger source kurtosis, k_s, is associated with greater resistance of the CMA to channel noise as long as the sources remain sub-Gaussian. However, a large value of k_s is widely known to inhibit CMA equalization [3], [8].

The issue of sensitivity to channel noise when the MMA is used with different sources is now addressed. Consider first the MMA with sources with $E[s^4]>0$ for which $Z \triangleq Z_{r_-} = \gamma + E[s^4]/3$. A larger γ or $E[s^4]$ (mainly γ) for a given source makes the MMA less sensitive to channel noise. For example, from the fifth column of Table I, V.34 ($k_s=1.66$) would be less sensitive to noise than V.29, which, in turn, less sensitive to noise than 4-PSK. Now consider the MMA with sources with $E[s^4]<0$ for which $Z \triangleq Z_{r_+} = \gamma + 2E[s^4]/3$. Since both $\gamma \geq 0$ and $Z>0$ are always true, a larger $|E[s^4]|$ corresponds to a smaller Z, and, consequently, greater sensitivity of the MMA to channel noise. These arguments will be confirmed by our simulation results in Section V (Figs. 2, 4 and 5).

V. COMPUTER SIMULATIONS

The ten two-dimensional symmetric signal constellations considered in Table I are quadrature phase-shift keying (QPSK) [Fig. 6.11(b), 14], 4-PSK [Fig. 6.11(a), 14], 8-PSK, square 16-QAM, 16-point V.29, Cross 32-QAM, square 256-QAM, Cross 128-QAM, as well as two 96-point V.34 modems with two different kurtoses by using constellation shaping [12]. The average powers required for V.34 with $k_s=1.23$ (with $E[s^4]<0$) and $k_s=1.66$ (with $E[s^4]>0$) are 84.1 and 46.96, respectively, where the transmit power efficiency of the latter was markedly increased. The channel, $c(t)=r(t,0.11)W(t)+0.8r(t-0.25T,0.11)W(t-0.25T) -0.4r(t-2T,0.11)W(t-2T)$, taken from [15], had a raised cosine pulse in a three-ray multipath environment, where $r(t,0.11)$ is a raised roll-off cosine pulse with the roll-off factor 0.11, and $W(t)$ is a rectangular truncation window spanning $[-3T,3T]$. Computer experiments were carried out using the *T/2*-spaced noisy channel model in [Fig. 5, 3] with each subchannel length $N_c=7$. Each subchannel output was rotated by 40°, and corrupted by a complex-valued additive white Gaussian noise such that different SNRs were adopted to verify the analytical results of the effect of channel noise on equalization convergence. Each of the two subequalizers had 11 complex tap weights ($N_f=11$) with five units of time delay. The tap weights of one subequalizer were initialized by setting the central tap weight to 1 and the others to zero, while all of the tap weights of the other subequalizer were set to zero. The performance index used to evaluate the performance was the ensemble-averaged ISI that measures the amount of residual ISI at the receiver, defined as $10\cdot\log_{10}\left(\left[\sum_k |h_k|^2 - \max(|h_k|^2)\right]\Big/\max(|h_k|^2)\right)$ over 100 independent runs. The values of the step-size parameter were chosen such that using the CMA and the MMA in the simulations generated about the same ensemble-averaged ISI in the steady state.

Figure 2 demonstrates that whereas the MMA using 16-QAM with SNR = 30 dB slightly outperformed the CMA in terms of residual ISI, the CMA outperformed the MMA in terms of residual ISI when SNR = 15 dB, because the CMA is less sensitive to channel noise than is the MMA. However, Fig. 2 also indicates that the MMA with square QAM is still relatively robust to channel noise. This is because the MMA with square QAM has a moderate value of $|E[s^4]|$, but a relatively large value of γ, and so the MMA with square QAM is still relatively robust against channel noise. Fig. 3 demonstrates that although the MMA using V.29 outperformed the CMA when SNR was 30 dB, this advantage associated with the MMA became less evident as SNR was decreased to 10 dB. When QPSK was used, the CMA outperformed the MMA when SNR was 30 dB, as presented in Fig. 4; the CMA had an even greater advantage over the MMA as SNR declined. This is because the MMA is most sensitive to channel noise when it is used with QPSK, which has the largest $|E[s^4]|$. Therefore, the CMA has an increasing advantage over the MMA as SNR becomes smaller when QPSK is used. Figure 5 indicates that although the CMA using Cross QAM significantly outperformed the MMA using cross QAM in terms of ISI, the MMA was highly resistant to channel noise when Cross QAM was used owing to its extremely small value of $|E[s^4]|$. Nevertheless, the CMA appears to be a little less vulnerable to channel noise than does the MMA when Cross QAM is used. Accordingly, for both square QAM and cross QAM, although the CMA is more resistant to channel noise than is the MMA, this advantage is relatively modest if SNR decreases. Finally, Fig. 6 demonstrates that when the CMA uses V.34 with a larger value of k_s, it is less sensitive to channel noise. However, a large value of k_s inhibits CMA equalization.

VI. CONCLUSIONS

The main results of this paper are summarized as follows. 1) The stationary points of both the CMA and the MMA move closer to the origin as SNR becomes smaller. 2) The CMA is less sensitive to channel noise than is the MMA in terms of blind equalization for all possible sources (see Figs. 2, 4 and 5). 3) The fourth-order statistic of the sources, which is critical to the carrier phase recovery of the MMA, turns out to make the MMA more vulnerable to additive channel noise than the CMA. 4) The MMA with square QAM and cross QAM is still relatively robust to channel noise. Additionally, when the MMA is used with sources with a positive fourth-order statistic (such as 4-PSK and V.29 modem), it still outperforms the CMA in terms of equalization convergence and carrier phase recovery when noise is present (see Fig. 3). 5) When the CMA is used with different sources, a larger source kurtosis corresponds to lower sensitivity of the CMA to channel noise (see Fig. 6). However, a large value of the source kurtosis is known to inhibit CMA equalization.

VII. ACKNOWLEDGEMENT

This work was supported by the National Science Council (NSC), Taiwan, R.O.C. under contract NSC 99-2221-E-030-010-MY2.

VIII. REFERENCES

[1] D. N. Godard, "Self-recovering equalization and carrier tracking in two-dimensional data communication system." *IEEE Trans. Commun.*, vol. 28, pp.1867-1875, Nov. 1980.

[2] J. R. Treichler and M. G. Larimore, "New Processing Techniques Based on the Constant Modulus Algorithm," *IEEE Trans. Acoust.*, Speech, *Signal Process.*, vol. ASSP-33, pp.420-431, Apr. 1985.

[3] C. R. Johnson, Jr., P. Schniter, T. J. Endres, J. D. Behm, D. R. Brown, and R. A. Casas, "Blind equalization using the constant modulus criterion: A review," *Proc. IEEE*, vol. 86, pp.1927-1950, Oct. 1998.

[4] J. R. Treichler, M. G. Larimore, and J. C. Harp, "Practical blind demodulators for high-order QAM signals," *Proc. IEEE*, vol. 86, pp. 1907-1925, Oct. 1998.
[5] K. Wesolowski, "Analysis and properties of the modified constant modulus algorithm for blind equalization," *European Trans. Telecommun.*, vol. 3, pp. 225-230, May-June 1992.
[6] J. Yang, J.-J. Werner, and G. A. Dumont, "The multimodulus blind equalization and its generalized algorithms," *IEEE J. Sel. Areas in Commun.*, vol. 20, pp. 997-1015, June 2002.
[7] J.-T. Yuan and K.-D. Tsai, "Analysis of the Multimodulus Blind equalization Algorithm in QAM Communication Systems," *IEEE Trans. Commun.*, vol. 53, pp. 1427-1431, Sept. 2005.
[8] J.-T. Yuan and T.-C. Lin, "Equalization and Carrier Phase Recovery of CMA and MMA in Blind Adaptive Receivers," *IEEE Trans. Signal Process.*, vol. 58, pp. 3206-3217, June 2010.
[9] I. Fijalkow, A. Touzni, and J. R. Treichler, "Fractionally spaced equalization using CMA: Robustness to channel noise and lack of disparity," *IEEE Trans. Signal Process.*, vol. 45, pp. 56-66, Jan. 1997.
[10] W. Chung and J. LeBlanc, "The local minima of fractionally-spaced CMA blind equalizer cost function in the presence of channel noise," *Proc. IEEE Int. Conf. Acoustics, Speech and Signal Process.*, 1998, pp. 3345-3348.
[11] ITU-T Recommendation V.29 – 9600 bits per second modem standardized for use on point-to-point 4-wire leased telephone-type circuits, 1988.
[12] C. E. D. Sterian, "The constellation-shaping algorithm using closed-form expressions for the number of ring combinations," *IEEE Trans. Commun.*, vol. 47, pp. 1462-1465, Oct. 1999.
[13] W. Chung and C. R. Johnson, Jr., "Characterization of the regions of convergence of CMA adapted Blind Fractionally Spaced Equalizer," *Proc. of the Thirty-Second Asilomar Conference Conf. on Signals, Systems and Computers*, 1998. pp. 493-497.
[14] S. Haykin, *Communication Systems*, John Wiley & Sons, 2001, 4th edition.
[15] Y. Li and Z. Ding, "Global convergence of fractionally spaced Godard (CMA) adaptive equalizers," *IEEE Trans. Signal Process.*, vol. 44, pp. 818-826, Apr. 1996.

TABLE I STATISTICS OF SOME IMPORTANT PARAMETERS FOR ALL CONSTELLATIONS CONSIDERED IN THIS WORK

Sources	$E[s^4]$	γ	Z_r	Z_{r_y}	k_s
4-PSK	1	0	0.5	0.333	1
QPSK	-1	1	0.5	0.333	1
8-PSK	0	0.5	0.5	0.5	1
16-QAM	-0.68	1	0.66	0.547	1.32
V.29	0.518	0.45	0.709	0.623	1.418
Cross 32-QAM	-0.19	0.75	0.655	0.5902	1.3819
Cross 128-QAM	-0.1814	0.762	0.671	0.641	1.343
256-QAM	-0.6047	1	0.698	0.597	1.395
V.34 (k_s=1.23)	-0.2266	0.726	0.615	0.577	1.23
V.34 (k_s=1.66)	0.2243	0.714	0.831	0.793	1.66

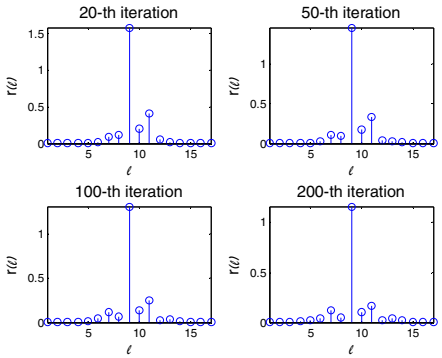

Fig. 1. Simulations results displaying how each non-zero component of the combined channel-equalizer vector **h** dynamically evolves during the blind equalization process at various iterations.

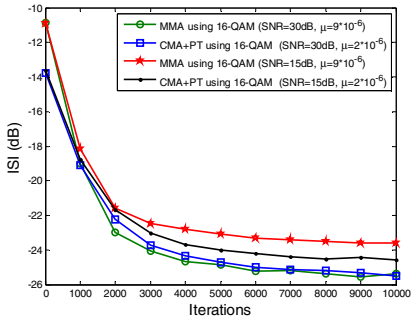

Fig. 2. A comparison of 100 ensemble-averaged ISI between CMA and MMA using 16-QAM with two different SNRs.

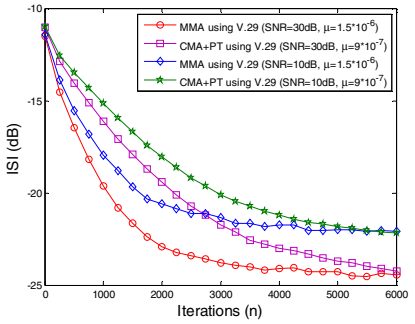

Fig. 3. A comparison of 100 ensemble-averaged ISI between CMA and MMA using V.29 with two different SNRs.

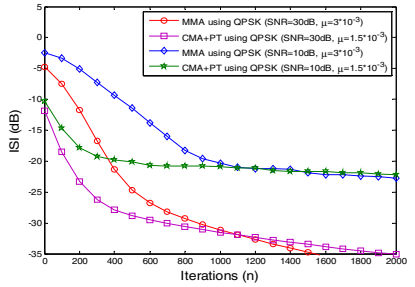

Fig. 4. A comparison of 100 ensemble-averaged ISI between CMA and MMA using QPSK with two different SNRs.

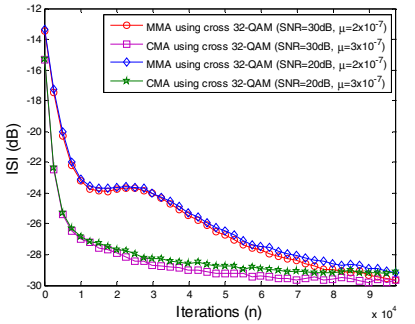

Fig. 5. A comparison of 100 ensemble-averaged ISI between CMA and MMA using cross 32-QAM with two different SNRs.

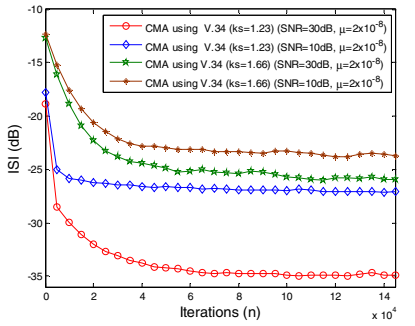

Fig. 6. A comparison of residual ISI of CMA with V.34 with two different kurtosis and two different SNRs.